J. Fluid Mech. (1998), *vol.* 354, *pp.* 345–356. Printed in the United Kingdom

© 1998 Cambridge University Press

Effects of stratification on quasi-geostrophic inviscid equilibria

By WILLIAM J. MERRYFIELD
Institute of Ocean Sciences, Sidney, B.C., Canada

(Received 24 September 1996 and in revised form 5 September 1997)

Inviscid equilibrium mean flows over topography are considered for continuously stratified quasi-geostrophic models, in contrast to previous work which has dealt with two-layer models. From the constraint of maximum entropy, an equation for the equilibrium mean flow is derived. Analytical solutions are obtained for uniform and piecewise-constant stratifications. With increasing stratification, the mean streamfunction becomes increasingly bottom intensified. Bottom trapping becomes ever more pronounced on smaller scales, but can remain significant even on the largest scales. When boundary temperature is uniform, transport is shown to be independent of stratification, other factors being equal. Although two-layer models share this property, they represent poorly the energetics of the continuous system when bottom trapping is significant.

1. Introduction

The inviscid equilibria of quasi-geostrophic flows can be characterized analytically using methods of statistical mechanics. Interest in such equilibria has heightened recently because of their relevance to certain eddy parameterizations for coarse-resolution ocean circulation models. The premise underlying these parameterizations is that eddies tend to restore toward inviscid equilibrium flows which are acted upon by forcing and dissipation. This equilibration tendency is represented by prescribing that unresolved eddies drive flows up entropy gradients, i.e. maximize entropy production (Holloway 1992; Kazantsev, Sommeria & Verron 1997).

To date, these parameterizations have considered barotropic equilibria only, and omitted effects of stratification. This is principally due to ignorance about the nature of stratified equilibria. Clearly, it is desirable to include such effects, as stratification is an important influence on ocean circulation. Except for two-layer models, expressions for stratified inviscid equilibria have not previously been available. The objective of this paper is to provide expressions for such flows, and to describe their properties.

Inviscid equilibria of two-layer models are reviewed in §2. In §3 an equation describing equilibrium mean flows in continuously stratified models is derived, and analytical solutions are obtained. The relationship between the two-layer and continuously stratified results is discussed in §4, and conclusions are presented in §5.

2. Inviscid equilibria of two-layer models

The dynamics of quasi-geostrophic layer models are described by

$$\frac{\partial q_i}{\partial t} + J(q_i, \psi_i) = 0, \qquad i = 1, \ldots, M, \tag{2.1}$$

https://doi.org/10.1017/S0022112097007684 Published online by Cambridge University Press

where M is the number of layers, q_i and ψ_i are the potential vorticity and streamfunction in layer i, and $J(A,B) = \partial(A,B)/\partial(x,y)$ is the Jacobian operator with respect to Cartesian coordinates (x,y). Salmon, Holloway & Hendershott (1976) (henceforth SHH) considered inviscid equilibria for models having $M = 1$, for which $q = \nabla^2\psi + \beta y + h$, and $M = 2$, for which

$$q_1 = \nabla^2\psi_1 + \beta y + F_1(\psi_2 - \psi_1), \tag{2.2a}$$

$$q_2 = \nabla^2\psi_2 + \beta y - F_2(\psi_2 - \psi_1) + h \tag{2.2b}$$

where $f = f_0 + \beta y$ is Coriolis parameter, ∇ is the horizontal gradient operator, $F_i = f_0^2/g'H_i$, where H_i is mean thickness of layer i and g' is reduced gravity, and $h = f_0(H - H_0)/H_M$, where H is total depth and H_0 is mean total depth. This paper concentrates on effects of topography and neglects latitudinal variations in f.

Equations (1) conserve total energy

$$E = \frac{1}{2}\iint\left[\sum_{i=1}^{M}\frac{H_i}{H_0}|\nabla\psi_i|^2 + \sum_{i=1}^{M-1}\frac{f_0^2}{g_i'H_0}(\psi_{i+1} - \psi_i)^2\right]\,\mathrm{d}x\,\mathrm{d}y, \tag{2.3}$$

together with arbitrary moments of q for each layer. The theory of SHH accounts for conservation of E and the potential enstrophies

$$Q_i = \frac{1}{2}\iint q_i^2\,\mathrm{d}x\,\mathrm{d}y, \tag{2.4}$$

and is applicable when topography and initial conditions are random (Merryfield & Holloway 1996).† For one-layer models, the equilibrium flow has a steady component which obeys $\mu\bar{\psi} = \bar{q}$, where the overbars denote ensemble averages, and $\mu \equiv \alpha/\beta$ is the ratio of two Lagrange multipliers, whose values depend on E, Q and h. For doubly periodic domains, considered here for simplicity, the Fourier transform of this relation yields $\bar{\psi}_{\boldsymbol{k}} = h_{\boldsymbol{k}}/(\mu + k^2)$, where $\boldsymbol{k}$ is wave vector and $k = |\boldsymbol{k}|$. Mean flows thus are correlated with topography in the sense of anticyclonic circulation over topographic elevations.

The expressions derived by SHH for mean flows in two-layer models are rewritten here in simplified form. The mean streamfunctions are

$$\bar{\psi}_{1,\boldsymbol{k}} = \frac{F_1 h_{\boldsymbol{k}}}{\Lambda}, \qquad \bar{\psi}_{2,\boldsymbol{k}} = \frac{(k^2 + F_1 + \mu_1)h_{\boldsymbol{k}}}{\Lambda}, \tag{2.5a}$$

where

$$\Lambda \equiv k^2(k^2 + F_1 + F_2) + \mu_1(k^2 + F_2) + \mu_2(k^2 + F_1) + \mu_1\mu_2, \tag{2.5b}$$

and $\mu_i \equiv \alpha/\beta_i$. The Lagrange multipliers α and β_i depend on E, Q_i, F_i and h, as described in Appendix A.

These solutions have several notable properties. Using (2.2) it is straightforward to show that the Fourier transforms of (2.5*a*,*b*) are equivalent to

$$\mu_i\bar{\psi}_i = \bar{q}_i. \tag{2.6}$$

As for $M = 1$, mean streamfunction is correlated with topography, the single-layer solution being recovered as $H_1 \to 0$ ($F_1 \to \infty$). As g' increases, the F_i decrease, and

† A theory that accounts for higher-order invariants has been developed by Miller (1990) and Robert & Sommeria (1991).

https://doi.org/10.1017/S0022112097007684 Published online by Cambridge University Press

the mean flow becomes increasingly trapped in the bottom layer for wavenumbers $k \gtrsim (F_1 + \mu_1)^{-1/2}$. This implies enhanced trapping on scales less than $(H_0/H_2)^{1/2}$ times the Rossby deformation radius $L_D = [g' H_1 H_2 / f_0^2 H_0]^{1/2}$ for $\mu_1 \lesssim F_1$, and on scales less than $\mu_1^{-1/2}$ for $\mu_1 \gtrsim F_1$. If $\mu_1 = \mu_2 \equiv \mu$, the mean transport streamfunction $\bar{\Psi} = \sum_i H_i \bar{\psi}_i$ is independent of g', and equal to its barotropic value $H_0 \bar{\psi}$. Finally, $\bar{\psi}$ remains partially bottom trapped even on the largest scales ($k \to 0$) for finite stratification $g' > 0$, with ratio $F_1/(F_1 + \mu_1)$ of upper to lower mean flow. For given μ_1, this effect becomes increasingly pronounced with increasing g'.

3. Inviscid equilibria of continuously stratified models

The two-layer models described in §2 are extremely simple representations of stratified quasi-geostrophic flow. Models allowing continuous dependence on depth z would be more realistic. The results quoted in §2 suggest patterns of behaviour for such systems, such as enhanced bottom trapping of mean flows on horizontal scales smaller than L_D. However, a more accurate and general description can be achieved by considering the continuously stratified case explicitly.

The continuously stratified problem is approached here by obtaining an equation for inviscid equilibrium $\bar{\psi}$ from the maximum-entropy constraint. Illustrative analytical solutions are then found for uniform and piecewise-constant stratification.

The maximum-entropy mean flows are obtained by the procedure illustrated in Salmon (1982) and in the Appendix of Holloway (1992). In the limit of continuous depth variation, the governing equation (2.1) becomes

$$\frac{\partial q}{\partial t} + J(\psi, q) = 0, \tag{3.1}$$

with $q(x, y, z)$ and $\psi(x, y, z)$ related by

$$q = \nabla^2 \psi + \frac{\partial}{\partial z} \left[\frac{f_0^2}{N^2(z)} \frac{\partial \psi}{\partial z} \right], \tag{3.2}$$

where N is Brunt–Väisälä frequency and z is depth. Equation (3.2) assumes nearly uniform density, as in the oceans, and constant Coriolis parameter f_0 (e.g. Pedlosky 1987, §6.8). The top and bottom boundary conditions are that velocities normal to the boundaries vanish. This implies $w = 0$ at the upper boundary and $w = \boldsymbol{u} \cdot \nabla(H)$ at the lower boundary, for horizontal velocity $\boldsymbol{u} = (-\partial_y \psi, \partial_x \psi)$ and vertical velocity

$$w = \left(\frac{\partial}{\partial t} + \boldsymbol{u} \cdot \nabla \right) \left[-\frac{f_0}{N^2(z)} \frac{\mathrm{d}\psi}{\mathrm{d}z} \right]. \tag{3.3}$$

The expression in square brackets represents vertical displacement of isotherms (constant temperature surfaces). For simplicity, it is assumed in this section that such surfaces are tangent to the boundaries. This represents the continuously stratified ($M \to \infty$) limit of the layer models of §2. The more general case in which isotherms may intersect the boundaries is considered in Appendix B.

With temperature uniform on the boundaries, the quadratic invariants are energy,

$$E = \frac{1}{2} \iiint \left\{ |\nabla \psi|^2 + \frac{f_0^2}{N^2(z)} \left(\frac{\partial \psi}{\partial z} \right)^2 \right\} \mathrm{d}x \, \mathrm{d}y \, \mathrm{d}z, \tag{3.4}$$

https://doi.org/10.1017/S0022112097007684 Published online by Cambridge University Press

and potential enstrophy at each depth,

$$\mathrm{d}Q(z) = \tfrac{1}{2}\,\mathrm{d}z \iint q^2\,\mathrm{d}x\,\mathrm{d}y. \tag{3.5}$$

The objective is to find $\psi(z)$ which maximizes entropy $S = -\int \mathrm{d}\boldsymbol{Y}\ p\ \log p$, subject to constraints imposed by the constant E and $\mathrm{d}Q(z)$, and by normalization of total probability to unity. Here, $\boldsymbol{Y}$ is state vector (a list of the dependent variables), and p is probability. The state of maximum S can be specified by requiring that the variation of S with respect to probability vanish. Introducing Lagrange multipliers α, $\beta(z)$ and η, whose values are determined by the constraints, leads to

$$\delta \int \mathrm{d}\boldsymbol{Y} \left[p\ \log p + \alpha E p + \int_0^{H_0} \beta(z)\mathrm{d}Q(z)p + \eta p \right] = 0, \tag{3.6}$$

which is satisfied for

$$\log p + \alpha E + \int_0^{H_0} \beta(z)\mathrm{d}Q(z) + \eta = 0, \tag{3.7}$$

or

$$p = \exp(-1-\eta)\exp\left\{ -\int_0^{H_0} \mathrm{d}z \left[\alpha \frac{\mathrm{d}E}{\mathrm{d}z} + \beta(z)\frac{\mathrm{d}Q}{\mathrm{d}z} \right] \right\}. \tag{3.8}$$

The Fourier modes for the ensemble-mean streamfunction can now be found from

$$\bar{\psi}_{\boldsymbol{k}}(z) = \int_{-\infty}^{\infty} \psi_{\boldsymbol{k}}(z) p[\psi_{\boldsymbol{k}}(z)]\mathrm{d}\psi_{\boldsymbol{k}}(z), \tag{3.9}$$

where p is given by (3.8), with

$$\frac{\mathrm{d}E}{\mathrm{d}z} = \frac{1}{H_0} \sum_{\boldsymbol{k}} \left\{ k^2 |\psi_{\boldsymbol{k}}|^2 + \frac{f_0^2}{N^2(z)} \left| \frac{\mathrm{d}\psi_{\boldsymbol{k}}}{\mathrm{d}z} \right|^2 \right\}, \tag{3.10}$$

$$\frac{\mathrm{d}Q}{\mathrm{d}z} = \frac{1}{H_0} \sum_{\boldsymbol{k}} \left| -k^2\psi_{\boldsymbol{k}} + \frac{\mathrm{d}}{\mathrm{d}z}\left[\frac{f_0^2}{N^2(z)} \frac{\mathrm{d}\psi_{\boldsymbol{k}}}{\mathrm{d}z} \right] \right|^2. \tag{3.11}$$

Straightforward evaluation of (3.9) leads to

$$\bar{\psi}_{\boldsymbol{k}}(z) = \frac{\beta(z)\dfrac{\mathrm{d}}{\mathrm{d}z}\left[\dfrac{f_0^2}{N^2(z)} \dfrac{\mathrm{d}\bar{\psi}_{\boldsymbol{k}}}{\mathrm{d}z} \right]}{\alpha + \beta(z)k^2}, \tag{3.12}$$

or

$$\frac{\mathrm{d}}{\mathrm{d}z}\left[\frac{f_0^2}{N^2(z)} \frac{\mathrm{d}\bar{\psi}_{\boldsymbol{k}}}{\mathrm{d}z} \right] - \left[k^2 + \mu(z) \right] \bar{\psi}_{\boldsymbol{k}}(z) = 0, \tag{3.13}$$

where $\mu(z) \equiv \alpha/\beta(z)$. From the Fourier transform of (3.2), this is equivalent to $\mu(z)\bar{\psi}(z) = \bar{q}(z)$. From (3.3), the conditions of vanishing normal velocity and uniform temperature at the top and bottom boundaries imply

$$\frac{\mathrm{d}\bar{\psi}_{\boldsymbol{k}}}{\mathrm{d}z} = 0 \qquad \text{at} \qquad z = 0, \tag{3.14}$$

and

$$\frac{\mathrm{d}\bar{\psi}_{\boldsymbol{k}}}{\mathrm{d}z} = \frac{N^2}{f_0^2} H_0 h_{\boldsymbol{k}} \qquad \text{at} \qquad z = H_0. \tag{3.15}$$

https://doi.org/10.1017/S0022112097007684 Published online by Cambridge University Press

Before considering analytical solutions to (3.13)–(3.15)†, two properties of $\bar{\psi}_k$ are deduced from these equations. The first is that $|\bar{\psi}_k|$ increases uniformly with depth, provided $\mu > 0$. This can be shown by integrating (3.13) with respect to depth, which yields

$$\frac{f_0^2}{N^2(z)}\frac{\mathrm{d}\bar{\psi}_k}{\mathrm{d}z} = \int_0^z \left[k^2 + \mu(z')\right]\bar{\psi}_k(z')\mathrm{d}z'. \tag{3.16}$$

Because $\mathrm{d}\bar{\psi}_k/\mathrm{d}z = 0$ at $z = 0$, $\bar{\psi}_k$ and $\mathrm{d}\bar{\psi}_k/\mathrm{d}z$ at infinitesimal depth must have the same sign. An extension of this argument to finite depths indicates that $|\bar{\psi}_k|$ cannot change sign, and monotonically increases downward. The lower boundary condition (3.15) fixes the sign of $\bar{\psi}_k$ to that of h_k.

The second property is that for given uniform $\mu(z) = \mu$, $\bar{\Psi}_k$ is independent of stratification $N(z)$, and equal to the barotropic transport streamfunction, as for the two-layer model considered in §2. This can be shown by integrating (3.12) over depth:

$$\begin{aligned}\bar{\Psi}_k &= \int_0^{H_0} \bar{\psi}_k(z)\mathrm{d}z \\ &= \frac{1}{\mu + k^2}\int_0^{H_0} \frac{\mathrm{d}}{\mathrm{d}z}\left[\frac{f_0^2}{N(z)}\frac{\mathrm{d}\bar{\psi}_k}{\mathrm{d}z}\right]\mathrm{d}z \\ &= \frac{h_k}{\mu + k^2}H_0,\end{aligned} \tag{3.17}$$

where boundary conditions (3.14)–(3.15) have been employed in evaluating the integral.

3.1. *Constant N*

When N and μ are uniform, (3.13) has constant coefficients and is particularly easy to solve. The general solution is then $\bar{\psi}_k = a\mathrm{e}^{Kz} + b\mathrm{e}^{-Kz}$, with

$$K \equiv \frac{N}{f_0}(k^2 + \mu)^{1/2} = \frac{L_D}{H_0}(k^2 + \mu)^{1/2}, \tag{3.18}$$

where $L_D = H_0 N/f_0$ is Rossby radius for uniform N. Substituting this form into the boundary conditions determines a and b, yielding

$$\bar{\psi}_k(z) = \frac{h_k}{\mu + k^2} K H_0 \frac{\cosh Kz}{\sinh K H_0}. \tag{3.19}$$

For given μ and h_k, this defines a family of solutions in the dimensionless quantity KH_0, which measures the importance of stratification.

For weak stratification ($KH_0 \ll 1$), $\bar{\psi}_k$ approaches the one-layer barotropic solution, with $\bar{\psi}_k$ independent of z:

$$\bar{\psi}_k \to \frac{h_k}{\mu + k^2} \qquad \text{as} \qquad N \to 0. \tag{3.20}$$

† Solutions to the inverse Fourier transform of (3.13)–(3.15) are analogous to steady solutions of the three-dimensional heat equation with a decay term,

$$\frac{\partial T}{\partial t} = \frac{\partial^2 T}{\partial^2 x} + \frac{\partial^2 T}{\partial^2 y} + \frac{\partial}{\partial z}\left[\kappa(z)\frac{\partial T}{\partial z}\right] - \mu(z)T = 0$$

with an insulating top boundary and prescribed flux of heat at the lower boundary.

https://doi.org/10.1017/S0022112097007684 Published online by Cambridge University Press

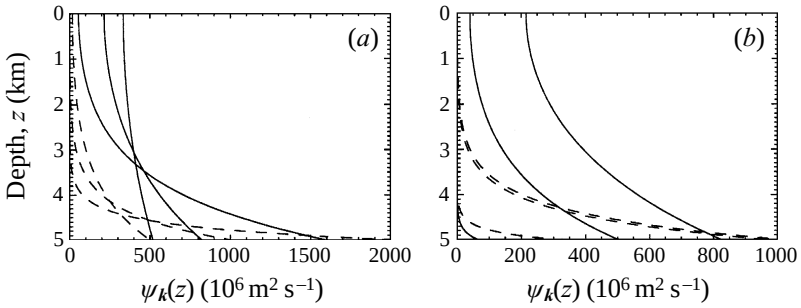


FIGURE 1. Equilibrium mean streamfunction $\bar{\psi}_{\boldsymbol{k}}(z)$, normalized to unit $h_{\boldsymbol{k}}$, for $H_0 = 5$ km and $f_0 = 10^{-4}$ s^{-1}. (*a*) $N = 0.4 \times 10^{-3}$ s^{-1}, 0.8×10^{-3} s^{-1}, and 1.6×10^{-3} s^{-1}, for $\mu^{-1/2} = 20$ km (solid) and 5 km (dashed). Surface-to-bottom variation increases with increasing N. The largest horizontal scales ($k \to 0$) are considered. (*b*) Horizontal scales $2\pi k^{-1} = 1000$ km, 100 km, and 10 km, for $\mu^{-1/2} = 20$ km (solid) and 5 km (dashed), and $N = 0.8 \times 10^{-3}$ s^{-1}. Amplitudes increase with increasing horizontal scale.

For strong stratification ($KH_0 \gg 1$),

$$\bar{\psi}_{\boldsymbol{k}} \to \frac{h_{\boldsymbol{k}}}{\mu + k^2} K H_0 \mathrm{e}^{-K(H_0 - z)} \qquad \text{as} \qquad N \to \infty, \tag{3.21}$$

so that the topographic influence on $\bar{\psi}_{\boldsymbol{k}}$ decays exponentially from the bottom with scale height K^{-1}. Figure 1 shows solutions for two choices of μ and different values of k and N.

The kinetic and available potential energies of the mean flow can be determined by substituting (3.19) into (3.10) and integrating over z. Kinetic energy, corresponding to the first term in (3.10), is

$$E_K = \sum_{\boldsymbol{k}} \frac{|h_{\boldsymbol{k}}|^2}{(\mu + k^2)^2} \frac{H_0 K}{4} k^2 \left(\frac{\sinh 2KH_0 + 2KH_0}{\sinh^2 KH_0} \right), \tag{3.22}$$

whereas available potential energy is

$$E_P = \sum_{\boldsymbol{k}} \frac{|h_{\boldsymbol{k}}|^2}{(\mu + k^2)^2} \frac{H_0 K}{4} (k^2 + \mu) \left(\frac{\sinh 2KH_0 - 2KH_0}{\sinh^2 KH_0} \right). \tag{3.23}$$

In the limit of weak stratification, the ratio of available potential to kinetic energy at wave vector $\boldsymbol{k}$ is

$$\left(\frac{E_P}{E_K} \right)_{\boldsymbol{k}} \to \frac{1}{3} \frac{(k^2 + \mu)^2}{k^2} L_D^2 \qquad (N \to 0), \tag{3.24}$$

which approaches infinity for horizontal scales much larger than $\mu^{-1/2}$, and $L_D^2/3$ for horizontal scales much smaller. For strong stratification,

$$\left(\frac{E_P}{E_K} \right)_{\boldsymbol{k}} \to \frac{(k^2 + \mu)}{k^2} \qquad (N \to \infty), \tag{3.25}$$

which approaches infinity for horizontal scales much larger than $\mu^{-1/2}$, and unity for horizontal scales much smaller.

3.2. *Piecewise-constant N*

Suppose now that N has distinct, uniform values over two ranges in depth divided by depth z_i. Equation (3.13) then has constant coefficients in each region and boundary

https://doi.org/10.1017/S0022112097007684 Published online by Cambridge University Press

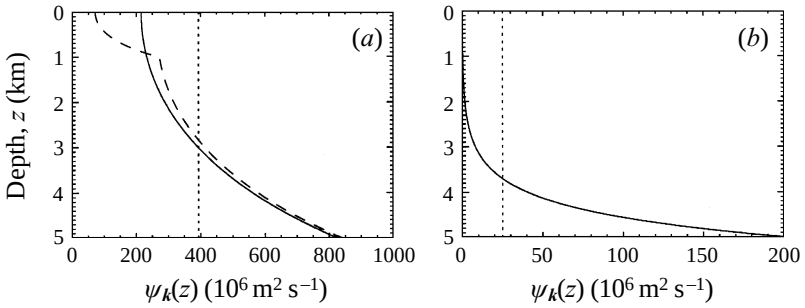


FIGURE 2. Equilibrium mean streamfunction $\bar{\psi}_k(z)$, normalized to unit h_k, for $N = 0$ (short-dashed), uniform $N = 0.8 \times 10^{-3}$ s^{-1} (solid), and piecewise-constant $N = 4.0 \times 10^{-3}$ s^{-1} ($0 < z < 1$ km), $N = 0.8 \times 10^{-3}$ s^{-1} ($z > 1$ km) (long-dashed). (*a*) $\mu^{-1/2} = 20$ km; (*b*) $\mu^{-1/2} = 5$ km.

conditions are (3.14)–(3.15), together with the conditions that $\bar{\psi}_k$ and $(f_0^2/N^2)\mathrm{d}\bar{\psi}_k/\mathrm{d}z$ be continuous at z_i. The derivation and form of the solution are outlined in Appendix C.

Figure 2 compares solutions having $N = 0$, constant N, and piecewise-constant N. Parameter values $z_i = 1$ km, $H_0 = 5$ km and $f_0 = 10^{-4}$ s^{-1} are approximately oceanic, and the piecewise-constant $N_1 = 4 \times 10^{-3}$ s^{-1} and $N_2 = 0.8 \times 10^{-3}$ s^{-1} correspond roughly to thermocline and abyssal values. The streamfunction on the largest scales ($k^{-1} \gg \mu^{-1/2}$) is shown. For $\mu^{-1/2} = 20$ km, the high-N 'thermocline' results in stronger attenuation of $\bar{\psi}$ in the uppermost few hundred metres; below, it has little influence. For $\mu^{-1/2} = 5$ km, the simulated thermocline has almost no effect because $\bar{\psi}$ is strongly attenuated already at thermocline depths.

4. Relation between two-layer and continuous solutions

This section examines the ability of the two-layer models of §2 to represent the continuous depth variation of $\bar{\psi}_k$ implied by (3.13). (Such comparisons are fairly standard for quasi-geostrophic models, and are applicable under conditions more general than the inviscid equilibria considered here.) For simplicity, constant N and constant μ are again considered.

For both the two-layer and continuous models, the transport streamfunction $\bar{\Psi}$ is independent of stratification and equal to barotropic $\bar{\Psi}$, as noted in §2 and §3. The vertical discretization implied by the two-layer formulation thus preserves the first moment of $\bar{\psi}_k$. However, significant differences arise for higher moments, such as the kinetic and available potential energies. These are given for two-layer models by Fourier components of the sums in (2.3), with $M = 2$ and $\bar{\psi}_k$ given by (2.5), and for continuous models by (3.22)–(3.23). The differences are most pronounced in the strongly stratified limit: $g' \to \infty$ ($F_i \to 0$) for two-layer models, and $N \to \infty$ ($KH_0 \gg 1$) for continuous models. In this limit, continuous $\bar{\psi}_k$ is trapped within approximately K^{-1} of the bottom in accordance with (3.21), whereas two-layer $\bar{\psi}_k$ is uniform within H_2 of the bottom, and vanishing above. Kinetic energies are related by

$$\left(\frac{\text{continuous } E_K}{\text{two-layer } E_K}\right)_k = \frac{KH_2}{2}, \tag{4.1}$$

and available potential energies by

$$\left(\frac{\text{continuous } E_P}{\text{two-layer } E_P}\right)_k = \frac{KH_2}{2}\frac{H_0^2}{H_1H_2}\frac{\mu + k^2}{F_1}. \tag{4.2}$$

https://doi.org/10.1017/S0022112097007684 Published online by Cambridge University Press

Because $KH_0 \gg 1$ for strong stratification, E_K is much larger for continuous models than for two-layer models if $H_2 \sim O(H_0)$. Also, because $F_1 \to 0$ in this limit and $H_0^2/H_1H_2 \geqslant 4$, E_P for continuous models is relatively larger still.

For continuous models, the ratio of mean-flow kinetic to available potential energy at wave vector $\boldsymbol{k}$, given by (3.25), remains finite in the strongly stratified limit. By contrast, for two-layer models,

$$\left(\frac{E_P}{E_K}\right)_{\boldsymbol{k}} = \frac{H_1H_2}{H_0^2}\frac{F_1}{k^2}, \tag{4.3}$$

which for fixed $\boldsymbol{k}$ becomes arbitrarily small as stratification g' ($\propto F_1^{-1}$) increases.

These qualitative differences can be traced to the inability of two-layer models to resolve the exponential surfaceward decay of $\bar{\psi}_{\boldsymbol{k}}$ when $KH_0 \gg 1$. For example, from (4.1) their kinetic energies become comparable only when $H_2 \approx K^{-1}$, in which case the scale length for upward decay of $\bar{\psi}_{\boldsymbol{k}}$ is crudely resolved by the two-layer, piecewise-constant representation. Such a correspondence cannot simultaneously be achieved for the respective potential energies. This is because the definition of available potential energy involves a vertical derivative of $\bar{\psi}_{\boldsymbol{k}}$. The inaccuracy of the two-layer formulation in representing this derivative attenuates two-layer E_P by a factor of order $(\mu + k^2)/F_1$, apparent in (4.2) and (4.3).

5. Discussion and conclusions

The solutions for stratified inviscid equilibria presented here could lead to improvements to an eddy parameterization proposed by Holloway (1992) and implemented in ocean circulation models (Alvarez *et al.* 1994; Eby & Holloway 1994; Fyfe & Marinone 1995; Holloway, Sou & Eby 1995; Sou, Holloway & Eby 1996; Pal & Holloway 1996). The parameterization represents entropy generation due to unresolved eddies by a term $A\nabla^n(\boldsymbol{u}-\boldsymbol{u}^*)$ replacing the viscous operator in the equations of motion. Here A is a coefficient, $n = 0$ or 2, and $\boldsymbol{u}^*$ is a maximum-entropy mean flow, which has been determined from barotropic $\bar{\psi}_{\boldsymbol{k}}$, given by the Fourier transform of (3.20), with $k \to 0$. The quantity μ in (3.20) has been interpreted as the inverse square of an eddy length scale.

Models using the Holloway (1992) parameterization typically have adopted values for $\mu^{-1/2}$ in the range of 5 to 10 km, whereas typical Rossby radii are around 10 km at subpolar latitudes and 20–40 km at midlatitudes (Emery, Lee & Magaard 1984). On scales coarser than $\mu^{-1/2}$, the dimensionless stratification parameter of §3.1 is approximately $KH_0 \approx L_D/\mu^{-1/2}$. Thus $KH_0 \gtrsim 1$ for parameters representative of ocean models, suggesting significant bottom intensification of $\boldsymbol{u}^*$, which could be taken into account in the Holloway (1992) parameterization.

The eddy parameterization of Kazantsev *et al.* (1997) is based on an entropy maximization procedure developed from the Robert & Sommeria (1991) theory of inviscid equilibria, and reduces to that of Holloway (1992) in the limits of statistical homogeneity and small Rossby number. As yet, it has been formulated only for unstratified quasi-geostrophic models. Based on the results presented here, this parameterization as well might benefit from accounting for stratification.

The procedure for finding inviscid equilibrium $\bar{\psi}_{\boldsymbol{k}}$ in §3 is incomplete in that $\mu(z)$ is not solved for. A full solution would specify $\mu(z)$, together with statistics of the fluctuating component of flow, as functions of topography h and the invariants E and $Q(z)$. While this would ultimately be desirable, the present treatment serves to illustrate some of the basic properties of stratified equilibrium mean flows.

https://doi.org/10.1017/S0022112097007684 Published online by Cambridge University Press

This work was supported by the Office of Naval Research (N00014-92-J-1775) and a Fellowship from the NOAA Postdoctoral Program in Climate and Global Change. Greg Holloway, Rick Salmon and an anonymous referee are thanked for suggesting improvements to the manuscript.

Appendix A. Determination of Lagrange multipliers for two-layer models

The Lagrange multipliers α and β_i, $i = 1, 2$, are determined by†

$$E = \sum_{\boldsymbol{k}} \frac{F}{\alpha \Lambda} \left[\mu_1(k^2 + F_2) + \mu_2(k^2 + F_1) + \mu_1\mu_2\right] + \frac{|h_{\boldsymbol{k}}|^2}{\Lambda^2}\left[\frac{H_1}{H_0}k^2F_1^2 + \frac{H_2}{H_0}k^2(k^2 + F_1 + F_2) + F(k^2 + \mu_1)^2\right], \tag{A 1}$$

$$Q_1 = \sum_{\boldsymbol{k}} \frac{\mu_1 F_1}{\alpha \Lambda}\left[\mu_2(k^2 + F_1) + k^2(k^2 + F_1 + F_2)\right] + \frac{|h_{\boldsymbol{k}}|^2}{\Lambda^2}\mu_1^2F_1^2, \tag{A 2}$$

$$Q_2 = \sum_{\boldsymbol{k}} \frac{\mu_2 F_2}{\alpha \Lambda}\left[\mu_1(k^2 + F_2) + k^2(k^2 + F_1 + F_2)\right] + \frac{|h_{\boldsymbol{k}}|^2}{\Lambda^2}\mu_2^2(k^2 + F_1 + \mu_1)^2, \tag{A 3}$$

where $F = f_0^2/g'H_0$, and Λ is given by (2.5*b*). In each equation, the first grouping of terms corresponds to fluctuating flow spectra, and the second grouping to mean flow spectra. Equations (A1)–(A3) can be inverted straightforwardly for α and β_i by iterating from an initial guess via a bisection procedure.

Appendix B. Inviscid equilibria for non-uniform boundary temperature

The results in §3 are generalized here to the case in which isotherms may intersect the top and bottom boundaries. The more general boundary conditions implied by (3.3) are

$$\frac{\partial \Theta_0}{\partial t} + J(\psi_0, \Theta_0) = 0, \tag{B 1}$$

$$\frac{\partial \Theta_1}{\partial t} + J(\psi_1, \Theta_1) = 0, \tag{B 2}$$

where $\psi_0 = \psi(x, y, z = 0)$ and $\psi_1 = \psi(x, y, z = H_0)$, and

$$\Theta_0 = -\frac{f_0^2}{N^2(0)}\frac{\partial \psi}{\partial z}\Big|_{z=0}, \tag{B 3}$$

$$\Theta_1 = -\frac{f_0^2}{N^2(H_0)}\frac{\partial \psi}{\partial z}\Big|_{z=H_0} - H_0 h, \tag{B 4}$$

are proportional to the temperature anomalies at the boundaries. Equations (B 1)–(B 2) give rise to an additional pair of quadratic invariants,

$$\Gamma_0 = \iint \Theta_0^2 \,\mathrm{d}x\,\mathrm{d}y, \qquad \Gamma_1 = \iint \Theta_1^2 \,\mathrm{d}x\,\mathrm{d}y, \tag{B 5a, b}$$

† Here, α and β_i are defined slightly differently than in SHH. Denoting the SHH Lagrange multipliers by α_s, β_{is}, $\alpha = 2\alpha_s$ and $\beta_i = 2\beta_{is}/F_i$.

https://doi.org/10.1017/S0022112097007684 Published online by Cambridge University Press

so that equation (3.7) for probability density becomes

$$\log p + \alpha E + \int_0^{H_0} \beta(z)\mathrm{d}Q(z) + \gamma_0\Gamma_0 + \gamma_1\Gamma_1 + \eta = 0, \tag{B 6}$$

where γ_0 and γ_1 are the Lagrange multipliers associated with Γ_0 and Γ_1.

Prior to expressing p as a function of Θ_0, Θ_1 and ψ, the energy invariant (3.4) is rewritten using (B 3)–(B 4) and integration by parts as

$$E = \iint \left\{ -\psi_1(\Theta_1 - H_0 h) + \psi_0\Theta_0 - \int_0^{H_0} \psi q \, \mathrm{d}z \right\} \mathrm{d}x \, \mathrm{d}y. \tag{B 7}$$

Equations (3.5) and (B 3)–(B 7) then lead to

$$p = \exp(-1-\eta)\exp\left\{ -\iint \mathrm{d}x \, \mathrm{d}y \; \left[\gamma_0\Theta_0^2 + \alpha\psi_0\Theta_0 + \gamma_1\Theta_1^2 - \alpha\psi_1(\Theta_1 - H_0 h) + \int_0^{H_0} \mathrm{d}z \, (-\alpha\psi q + \beta(z)q^2) \right] \right\}. \tag{B 8}$$

Expressing ψ, Θ_0 and Θ_1 as Fourier expansions, and using (B 8) to evaluate (3.9) and analogous expressions for $\bar{\Theta}_0$, $\bar{\Theta}_1$ yields

$$\frac{\mathrm{d}}{\mathrm{d}z}\left[\frac{f_0^2}{N^2(z)} \frac{\mathrm{d}\bar{\psi}_{\boldsymbol{k}}}{\mathrm{d}z} \right] - \left[k^2 + \mu(z) \right] \bar{\psi}_{\boldsymbol{k}}(z) = 0, \tag{B 9}$$

with $\mu(z) \equiv \alpha/\beta(z)$ as before, and

$$\bar{\Theta}_{0,\boldsymbol{k}} = -v_0\psi_{0,\boldsymbol{k}}, \qquad \bar{\Theta}_{1,\boldsymbol{k}} = v_1\psi_{1,\boldsymbol{k}}, \tag{B 10a,b}$$

where $v_0 \equiv \alpha/2\gamma_0$ and $v_1 \equiv \alpha/2\gamma_1$. When $v_0 > 0$ and $v_1 > 0$, topographic bumps give rise to cold anomalies at the surface, and warm anomalies at the bottom, where isotherms are hence flatter than topography. Equations (10) translate into boundary conditions

$$\frac{\mathrm{d}\bar{\psi}_{\boldsymbol{k}}}{\mathrm{d}z} = \frac{N^2}{f_0^2} v_0 \bar{\psi}_{\boldsymbol{k}} \qquad \text{at} \qquad z = 0, \tag{B 11}$$

and

$$\frac{\mathrm{d}\bar{\psi}_{\boldsymbol{k}}}{\mathrm{d}z} = \frac{N^2}{f_0^2} \left[-v_1 \bar{\psi}_{\boldsymbol{k}} + H_0 h_{\boldsymbol{k}} \right] \qquad \text{at} \qquad z = H_0. \tag{B 12}$$

As in §3, $\bar{\psi}_{\boldsymbol{k}}$ is non-vanishing only when topography $h_{\boldsymbol{k}}$ is finite. For uniform N and μ, the solution is

$$\bar{\psi}_{\boldsymbol{k}}(z) = \frac{K\cosh Kz + v_0 \dfrac{N^2}{f_0^2} \sinh Kz}{K(v_0 + v_1)\dfrac{N^2}{f_0^2}\cosh KH_0 + \left[K^2 + (v_0 + v_1)\left(\dfrac{N^2}{f_0^2} \right)^2 \right] \sinh KH_0} \frac{N^2}{f_0^2} H_0 h_{\boldsymbol{k}}, \tag{B 13}$$

with K again given by (3.18).

If $v_0 = v_1 = 0$, surface temperature anomalies Θ_0 and Θ_1 vanish, and these results reduce to the special case of uniform boundary temperature considered in §3. Similarly, if $\mu(z) = 0$, potential vorticity q vanishes, and the results correspond to the surface quasi-geostrophic dynamics of Held *et al.* (1995), generalized to finite depth with topography.

https://doi.org/10.1017/S0022112097007684 Published online by Cambridge University Press

Appendix C. Solution of equation (3.13) for piecewise-constant N

Suppose $N = N_1$ for $0 \leqslant z < z_i$ and $N = N_2$ for $z_i < z < H$. In addition to (3.14)–(3.15), the boundary conditions on (3.13) are continuity of $\bar{\psi}_{\boldsymbol{k}}$ and $(f_0^2/N^2)\mathrm{d}\bar{\psi}_{\boldsymbol{k}}/\mathrm{d}z$ at $z = z_i$. The solution, assuming piecewise-constant μ, is of the form

$$\bar{\psi}_{\boldsymbol{k}}(z) = a_1 \mathrm{e}^{K_1 z} + b_1 \mathrm{e}^{-K_1 z}, \qquad 0 \leqslant z \leqslant z_i, \tag{C 1}$$

$$\bar{\psi}_{\boldsymbol{k}}(z) = a_2 \mathrm{e}^{K_2 z} + b_2 \mathrm{e}^{-K_2 z}, \qquad z_i \leqslant z \leqslant H, \tag{C 2}$$

where

$$K_i = \frac{N_i}{f_0}(k^2 + \mu_i)^{1/2}, \qquad i = 1, 2. \tag{C 3}$$

The four coefficients a_i and b_i are determined by the boundary conditions, yielding

$$\bar{\psi}_{\boldsymbol{k}}(z) = \frac{h_{\boldsymbol{k}}}{\Delta} K_2 H_0 \cosh K_1 z, \qquad 0 \leqslant z \leqslant z_i, \tag{C 4}$$

$$\bar{\psi}_{\boldsymbol{k}}(z) = \frac{h_{\boldsymbol{k}}}{\Delta} K_2 H_0 \left[\cosh K_1 z_i \cosh K_2(z - z_i) + \frac{K_1}{K_2}\frac{N_2^2}{N_1^2} \sinh K_1 z_i \sinh K_2(z - z_i)\right], \qquad z_i \leqslant z \leqslant H, \tag{C 5}$$

where

$$\Delta = \frac{f_0^2}{N_1^2} K_1 K_2 \sinh K_1 z_i \cosh K_2(H_0 - z_i) + \frac{f_0^2}{N_2^2} K_2^2 \cosh K_1 z_i \sinh K_2(H_0 - z_i). \tag{C 6}$$

REFERENCES

Alvarez, A., Tintore, J., Holloway, G., Eby, M. & Beckers, J. M. 1994 Effect of topographic stress on the circulation in the western Mediterranean. *J. Geophys. Res.* **99**, 16053–16064.

Eby, M. & Holloway, G. 1994 Sensitivity of a large-scale ocean model to a parameterization of topographic stress. *J. Phys. Oceanogr.* **24**, 2577–2588.

Emery, W. J., Lee, W. G. & Magaard, L. 1984 Geographic and seasonal distributions of Brunt-Väisälä frequency and Rossby radii in the North Pacific and North Atlantic. *J. Phys. Oceanogr.* **14**, 294–317.

Fyfe, J. & Marinone, G. 1995 On the role of unresolved eddies in a model of the residual currents in the central Strait of Georgia, B.C. *Atmos.-Ocean* **33**, 613–619.

Held, I. M., Pierrehumbert, R. T., Garner, S. T. & Swanson, K. T. 1995 Surface quasi-geostrophic dynamics. *J. Fluid Mech.* **282**, 1–20.

Holloway, G. 1992 Representing topographic stress for large-scale ocean models. *J. Phys. Oceanogr.* **22**, 1033–1046.

Holloway, G., Sou, T. & Eby, M. 1995 Dynamics of circulation of the Japan Sea. *J. Mar. Res.* **53**, 539–569.

Kazantsev, E., Sommeria, J. & Verron, J. 1997 Subgridscale eddy parameterization by statistical mechanics in a barotropic ocean model. *J. Phys. Oceanogr.* (to appear).

Merryfield, W. & Holloway, G. 1996 Inviscid quasi-geostrophic flow over topography: testing statistical mechanical theory. *J. Fluid Mech.* **309**, 85–91.

Miller, J. 1990 Statistical mechanics of Euler equations in two dimensions. *Phys. Rev. Lett.* **22**, 2137–2140.

Pal, B. K. & Holloway, G. 1996 Dynamics of circulation off the westcoast of Vancouver Island. *Cont. Shelf Res.* **16**, 1591–1607.

Pedlosky, J. 1987 *Geophysical Fluid Dynamics.* Springer.

Robert, R. & Sommeria, J. 1991 Statistical equilibrium states for two-dimensional flows. *J. Fluid Mech.* **229**, 291–310.

https://doi.org/10.1017/S0022112097007684 Published online by Cambridge University Press

Salmon, R. 1982 Geostrophic Turbulence. In *Topics in Ocean Physics, Proc. Intl Sch. Phys. 'Enrico Fermi', Varenna, Italy*, pp. 30–78.

Salmon, R., Holloway, G. & Hendershott, M. C. 1976 The equilibrium statistical mechanics of simple quasi-geostrophic models. *J. Fluid Mech.* **75**, 691–703 (referred to herein as SHH).

Sou, T., Holloway, G. & Eby, M. 1996 Effects of topographic stress on Caribbean Sea circulation. *J. Geophys. Res.* **101**, 16449–16453.

https://doi.org/10.1017/S0022112097007684 Published online by Cambridge University Press